Inorg. Chem. **2006**, *45*, 2461−2473

Acetylenic Carbon-13 Chemical Shift Tensors for Diphenylacetylene and (η^2-Diphenylacetylene)Pt(PPh_3)$_2$: A Solid-State NMR and Theoretical Study

Kristopher J. Harris,[†] Guy M. Bernard,[†] Chris McDonald,[†] Robert McDonald,[‡] Michael J. Ferguson,[‡] and Roderick E. Wasylishen*[,†]

Department of Chemistry and X-ray Crystallography Laboratory, University of Alberta, Edmonton, Alberta, T6G 2G2, Canada

Received September 9, 2005

The structure of (η^2-diphenylacetylene)Pt(PPh_3)$_2$, as well as those of its dichloromethane and benzene solvates, is determined via X-ray crystallography. An investigation of the chemical shift (CS) tensors of the ^{13}C-labeled carbons in Ph^{13}C≡^{13}CPh and (η^2-Ph^{13}C≡^{13}CPh)Pt(PPh_3)$_2$·(C_6H_6) is carried out via analysis of ^{13}C NMR spectra from stationary solid samples. The principal components of the CS tensors as well as their orientations with respect to the ^{13}C,^{13}C internuclear vector are determined. DFT calculations of these CS tensors are in close agreement with the experimental values. For diphenylacetylene (tolane), the orientations and principal-component magnitudes of the alkynyl carbon CS tensors are comparable to those for other alkynyl carbons, although the CS tensor is not axially symmetric in this case. Coordination to platinum causes a change in the CS tensor orientation and a net increase in the isotropic chemical shift, resulting from a significant increase in two principal components (δ_{11} and δ_{33}) while the third (δ_{22}) decreases only slightly. The measured carbon CS tensors in the platinum complex bear a striking similarity to those of the alkenyl carbons in *trans*-Ph(H)C═C(H)Ph, and a short theoretical discussion of these observations is presented.

1. Introduction

The field of unsaturated-ligand organometallic complexes continues to be an area of extensive research, mainly because of their unusual structures and useful catalytic properties.[1] Molecular complexes of platinum(0) and platinum(II) are important prototypes for the bonding of unsaturated carbon atoms to late transition metals.[2,3] A useful technique for characterizing these compounds has been their ^{13}C NMR spectra obtained in suitable solvents.[4] These studies have shown that, in general, coordination to platinum(II) results in an increased magnetic shielding for both alkenyl and alkynyl carbon nuclei.[4,5,6] Coordination to platinum(0) causes an increase in shielding for alkenyl carbons,[4,7] but a decrease in shielding for alkynyl carbons.[4,8] An NMR investigation of solid copper(I)−acetylene complexes spinning rapidly at the magic angle has also been performed by Walraff, who found that only small changes in the isotropic shielding occur upon bonding to copper.[9,10]

* To whom correspondence should be addressed. Phone: (780) 492-4336. Fax: (780) 492-8231. E-mail: Roderick.Wasylishen@ualberta.ca.
[†] Department of Chemistry.
[‡] X-ray Crystallography Laboratory.

(1) Mingos, D. M. P. Bonding of Unsaturated Organic Molecules to Transition Metals. In *Comprehensive Organometallic Chemistry*; Wilkinson, G., Ed.; Pergamon: Oxford, U.K., 1982; Vol. 3, pp 2−88.
(2) Hartley, F. R. Platinum. In *Comprehensive Organometallic Chemistry*; Wilkinson, G., Ed.; Pergamon: Oxford, U.K., 1982; Vol. 6, pp 471−736.
(3) Young, G. B. Platinum−Carbon π-Bonded Complexes. In *Comprehensive Organometallic Chemistry II*; Puddephatt, R. J., Ed.; Pergamon: Oxford, U.K., 1995; Vol. 9, pp 533−582.
(4) Mann, B. E.; Taylor, B. F. In *^{13}C NMR Data for Organometallic Compounds*; Maitlis, P. M., Stone, F. G. A., West, R., Eds.; Academic Press: London, 1981.
(5) For ease of discussion, the terms alkenyl and alkynyl carbon will be used to describe nuclei of the uncoordinated ligand and the corresponding nuclei in the complex, although in the latter case this does not correspond to a strict definition of the term.
(6) Cooper, D. G.; Powell, J. *Inorg. Chem.* **1976**, *15*, 1959−1968.
(7) Chaloner, P. A.; Davies, S. E.; Hitchcock, P. B. *Polyhedron* **1997**, *16*, 765−776.
(8) Boag, N. M.; Green, M.; Grove, D. M.; Howard, J. A. K.; Spencer, J. L.; Stone, F. G. A. *J. Chem. Soc., Dalton Trans.* **1980**, 2170−2181.
(9) Walraff, G. M. Ph.D. Thesis, University of Utah, Salt Lake City, UT, 1985.
(10) Bernard, G. M.; Wasylishen, R. E. NMR Studies of Ligand Nuclei in Organometallic Compounds—New Information from Solid-State NMR Techniques. In *Physical Organometallic Chemistry*; Gielen, M., Willem, R., Wrackmeyer, B., Eds.; John Wiley & Sons: West Sussex, U.K., 2002; Vol. 3, pp 165−205.

10.1021/ic051548f CCC: $33.50
Published on Web 02/22/2006

While the solution ^{13}C NMR studies mentioned above provide classificatory data and insight into the nature of ligand−metal bonding, only the isotropic portion of the chemical shifts are determined. Examining solid samples offers the opportunity to elucidate the orientation-dependent chemical shift (CS) tensor. Solid-state NMR (SSNMR) studies of slow-spinning samples have been used to elucidate the CS tensor principal components for the alkenyl carbons in a large series of platinum−alkene compounds.[11−15] In addition to principal-component magnitudes, the orientations of the alkenyl carbon CS tensors have been measured experimentally (with respect to the $^{13}C,^{13}C$ internuclear vector) for Zeise's salt,[16] a Pt(II) complex, as well as (η^2-$H_2C{=}CH_2$)Pt(PPh_3)$_2$,[16] and (η^2-*trans*-Ph(H)C=C(H)Ph)Pt(PPh_3)$_2$,[17] both Pt(0) complexes. Also, alkenyl carbon CS tensor orientations for selected cyclooctadiene and ethylene ligands in platinum, silver, rhodium, and copper organometallic complexes were calculated by Havlin et al.[13] A review of ^{13}C SSNMR investigations on a wealth of organometallic environments including assorted metal−olefin complexes, metallocenes, cyclopentadiene compounds, metal carbides, and fullerides, as well as surface-adsorbed olefins and acetylenes, has been compiled by Bernard and Wasylishen.[10]

To our knowledge, the principal components and orientation of a CS tensor for an alkynyl carbon η^2-bonded to a transition metal have never been reported.[5] Determination of such data would provide insights as to why the effect of η^2-bonding on the isotropic chemical shift is different for alkenyl and alkynyl carbons. In this article we report the characterization of alkynyl carbon CS tensors for the representative compound (η^2-diphenylacetylene)Pt(PPh_3)$_2$ (herein labeled PtDPA). Introduction of double ^{13}C labeling at the alkynyl carbon position allows analysis of spectra from stationary samples as homonuclear spin pairs, using the dipolar chemical-shift method.[18−21] The principal components of the carbon CS tensors, as well as their orientations relative to the $^{13}C,^{13}C$ internuclear vector (i.e., the alkynyl bond), are thus determined.

A complete structure for PtDPA has not previously been determined, although a preliminary X-ray study reported the space group and unit-cell parameters, but only a few bond lengths and angles.[22] To complete the structural information, we undertook a single-crystal X-ray diffraction study of PtDPA. Crystals of PtDPA as benzene and dichloromethane solvates, as well as without cocrystallized solvent, were readily isolated, and we report structural details for each form. Because of the favorable symmetry properties, the SSNMR data presented here was obtained from a crystal of the benzene solvate.

Alkynyl carbon CS tensors of unbound diphenylacetylene (DPA) are also determined using the dipolar chemical shift method on a doubly ^{13}C-labeled sample. The current investigation of DPA, in conjunction with data from PtDPA, allows a complete picture of the changes that η^2-bonding to platinum causes in the CS tensor of an alkynyl carbon. An assortment of alkynyl carbon CS tensors have previously been reported for compounds with a variety of substituents on the acetylenic carbons.[19,23−28] The alkynyl carbon CS tensor of DPA was reported during a preliminary investigation of DPA and PtDPA;[10] however, the presence of multiple solvate forms of PtDPA hindered completion of the study.

A theoretical investigation of the alkynyl carbon CS tensors of PtDPA and DPA is also presented. Numerous computational studies of transition metal complexes have been performed, and the area has been the subject of recent reviews by Dedieu,[29] as well as by Frenking and Fröhlich.[30] For both DPA and PtDPA, ambiguities in the CS tensor orientation resulting from the cylindrical symmetry of the dipolar interaction are resolved using DFT calculations. In addition, DFT calculations are used to investigate the nature of the relativistic effects on carbon CS tensors in the platinum complex.[31] Intuitive insight can be gained from theoretical investigations of CS tensors using, for example, the Cornwell approximation,[32−34] the DFT implementation of Schreckenbach and Ziegler,[35−37] or the individual gauges for atoms in molecules (IGAIM) method.[27,38,39] The DFT method of

(11) Huang, Y.; Gilson, D. F. R.; Butler, I. S. *J. Chem. Soc., Dalton Trans.* **1992**, 2881−2883.
(12) Gay, I. D.; Young, G. B. *Organometallics* **1996**, *15*, 2264−2269.
(13) Havlin, R.; McMahon, M.; Srinivasan, R.; Le, H.; Oldfield, E. *J. Phys. Chem. A* **1997**, *101*, 8908−8913.
(14) Ding, S.; McDowell, C. A. *Chem. Phys. Lett.* **1997**, *268*, 194−200.
(15) Challoner, R.; Sebald, A. *Solid State Nucl. Magn. Reson.* **1995**, *4*, 39−45.
(16) Bernard, G. M.; Wasylishen, R. E.; Phillips, A. D. *J. Phys. Chem. A* **2000**, *104*, 8131−8141.
(17) Bernard, G. M.; Wu, G.; Wasylishen, R. E. *J. Phys. Chem. A* **1998**, *102*, 3184−3192.
(18) VanderHart, D. L.; Gutowsky, H. S. *J. Chem. Phys.* **1968**, *49*, 261−271.
(19) Zilm, K. W.; Grant, D. M. *J. Am. Chem. Soc.* **1981**, *103*, 2913−2922.
(20) Power, W. P.; Wasylishen, R. E. *Annu. Rep. NMR Spectrosc.* **1991**, *23*, 1−77.
(21) Eichele, K.; Wasylishen, R. E. *J. Magn. Reson., Ser. A* **1994**, *106*, 46−56.
(22) Glanville, J. O.; Stewart, J. M.; Grim, S. O. *J. Organomet. Chem.* **1967**, *7*, P9−P10.
(23) Beeler, A. J.; Orendt, A. M.; Grant, D. M.; Cutts, P. W.; Michl, J.; Zilm, K. W.; Downing, J. W.; Facelli, J. C.; Schindler, M. S.; Kutzelnigg, W. *J. Am. Chem. Soc.* **1984**, *106*, 7672−7676.
(24) Pines, A.; Gibby, M. G.; Waugh, J. S. *Chem. Phys. Lett.* **1972**, *15*, 373−376.
(25) Cross, V. R.; Waugh, J. S. *J. Magn. Reson.* **1977**, *25*, 225.
(26) Bernard, G. M.; Wasylishen, R. E. *Solid State Nucl. Magn. Reson.* **2002**, *21*, 86−104.
(27) Wiberg, K. B.; Hammer, J. D.; Zilm, K. W.; Keith, T. A.; Cheeseman, J. R.; Duchamp, J. C. *J. Org. Chem.* **2004**, *69*, 1086−1096.
(28) Farrar, T. C.; Jablonsky, M. J.; Schwartz, J. L. *J. Phys. Chem.* **1994**, *98*, 4780−4786.
(29) Dedieu, A. *Chem. Rev.* **2000**, *100*, 543−600.
(30) Frenking, G.; Fröhlich, N. *Chem. Rev.* **2000**, *100*, 717−774.
(31) Autschbach, J.; Ziegler, T. Relativistic Computation of NMR Shieldings and Spin−Spin Coupling Constants. In *Encyclopedia of Nuclear Magnetic Resonance*; Grant, D. M., Harris, R. K., Eds.; John Wiley & Sons: Chichester, U.K., 2002; Vol. 9, pp 306−323.
(32) Cornwell, C. D. *J. Chem. Phys.* **1966**, *44*, 874.
(33) Grutzner, J. B. Chemical Shift Theory. Orbital Symmetry and Charge Effects on Chemical Shifts. In *Recent Advances in Organic NMR Spectroscopy*; Lambert, J. B., Rittner, R., Eds.; Norell Press: Landisville, NJ, 1987; pp 17−42.
(34) Dahn, H. *J. Chem. Educ.* **2000**, *77*, 905−909.
(35) Schreckenbach, G.; Ziegler, T. *J. Phys. Chem.* **1995**, *99*, 606−611.
(36) Schreckenbach, G. Ph.D. Thesis, University of Calgary, Calgary, AB, Canada, 1996.
(37) Schreckenbach, G.; Ziegler, T. *Int. J. Quantum Chem.* **1996**, *60*, 753−766.
(38) Wiberg, K. B.; Hammer, J. D.; Zilm, K. W.; Cheeseman, J. R.; Keith, T. A. *J. Phys. Chem. A* **1998**, *102*, 8766−8773.
(39) Wiberg, K. B.; Hammer, J. D.; Zilm, K. W.; Cheeseman, J. R. *J. Org. Chem.* **1999**, *64*, 6394−6400.

Schreckenbach and Ziegler is applied here to the CS tensor in the model compound (η^2-acetylene)Pt(PMe_3)$_2$ to clarify the effects of bonding on the CS tensor of an alkynyl carbon.

2. NMR: Background Theory and Conventions

In an NMR experiment, the nucleus is shielded from the applied magnetic field by the motion of neighboring electrons. It is well-known that this magnetic shielding can be described using a second rank tensor, σ.[40] We make the usual assumption that the tensor can be considered as symmetric across the lead diagonal.[40,41] When represented in a coordinate system known as the principal axis system (PAS), the tensor becomes diagonal (i.e., has only three nonzero elements). A symmetric shielding tensor is therefore fully described if both the magnitude of these three principal components and the orientation of the PAS in the molecular frame are known. By convention,[42] these elements are ordered from least to greatest shielding, $\sigma_{11} \leq \sigma_{22} \leq \sigma_{33}$, and their average is given by σ_{iso}. Magnetic shielding results in a deviation of the resonance frequency from that of a bare nucleus (e.g., C^{6+} for ^{13}C NMR), making it a difficult quantity to measure directly. Experiments are therefore simplified by measuring the difference in shielding from a reference compound, and this quantity is defined as the chemical shift (CS) and given the symbol δ.[43] The principal components of the CS tensor may be calculated from the corresponding elements of the magnetic shielding tensor and the isotropic shielding of a reference compound[42]

$$\delta_{ii}^{\text{sample}} = \frac{\sigma^{\text{ref}} - \sigma_{ii}^{\text{sample}}}{1 - \sigma^{\text{ref}}} \tag{1}$$

where σ^{ref} is taken as 184.1 ppm for the 300 K value of the standard ^{13}C reference, liquid TMS.[44] The CS tensor has the same PAS as the shielding tensor; its components are also labeled in order of least to greatest shielding, $\delta_{11} \geq \delta_{22} \geq \delta_{33}$, and the average of the elements is given by δ_{iso}.[42] A further parameter often useful in discussing CS tensors is the span, $\Omega = \delta_{11} - \delta_{33}$, which quantifies the total range over which the chemical shift varies. The frequency response of a nucleus depends on the orientation of the applied magnetic field in the PAS of the CS tensor. Components of the δ tensor can be determined from solid samples, relaxation studies, or solutes dissolved in liquid crystal solvents (samples dissolved in isotropic liquids yield δ_{iso}), but the PAS is generally difficult to ascertain without laborious single-crystal experiments.[43,45]

Nuclei in a molecule interact not only with the applied magnetic field, but also couple with magnetic fields generated by other nuclei in the sample. The through-space coupling is termed the direct-dipolar interaction, and its strength is quantified in the direct-dipolar coupling constant, which is given in hertz by[46]

$$R_{\text{DD}} = \left(\frac{\mu_0 \hbar}{8\pi^2}\right)\gamma_I \gamma_S \langle r_{IS}^{-3} \rangle \tag{2}$$

For a given I,S spin pair, R_{DD} depends on the distance between the nuclei (through r_{IS}) as well as the magnitude of their magnetic dipole moments (as represented in the γ_i's, known as the magnetogyric ratios). The frequency response of a dipolar-coupled spin pair depends on R_{DD} as well as the angle between the applied field and the internuclear $\vec{\mathbf{r}}_{IS}$ vector. This angular dependence averages to zero for both solutes in isotropic liquids and solids spinning rapidly at the magic angle so that the dipolar coupling has no effect on NMR spectra recorded under these conditions (provided only spin-1/2 nuclei are involved).

The magnetic dipole moments of the nuclei can induce a polarization of the electron spins, thus providing a second method of internuclear coupling. This indirect spin−spin coupling can also be quantified with a second rank tensor, **J**.[46,47] For the samples studied here, however, this (comparatively small)[48] angular dependence was overwhelmed by that of the direct-dipolar coupling (vide infra) so that only isotropic averages, J_{iso}, are reported. It should be noted however, that the full tensor form of **J** must often be taken into account, particularly for heavy nuclei.[46,47]

For the samples presented herein, ^{13}C NMR spectra of stationary samples under high-power ^1H decoupling may be considered to result from isolated ^{13}C spin pairs (vide infra). Applicable interactions for such a homonuclear spin pair are the dipolar and indirect couplings as well as the magnetic shielding of each nucleus. The strength of each interaction depends on the orientation of the applied magnetic field in each principal axis system. This dependence on multiple frames of reference encodes the relative orientation of each frame into the NMR spectrum of a stationary powder. The dipolar chemical-shift method is designed to yield the magnitude of R_{DD}, the elements of each CS tensor, and the orientation of each CS tensor with respect to the internuclear vector. This method has proven useful in a large number of studies and has been described many times.[16−21] See refs 17 and 20 for a description of the method in terms of the nomenclature and conventions used here.

A particularly efficient method for reporting the angular information is to use the internuclear vector of the spin pair

(40) Anet, F. A. L.; O'Leary, D. J. *Concepts Magn. Res.* **1991**, *3*, 193-214.
(41) Schneider, R. F. *J. Chem. Phys.* **1968**, *48*, 4905−4909.
(42) Mason, J. *Solid State Nucl. Magn. Reson.* **1993**, *2*, 285−288.
(43) Grant, D. M. Chemical Shift Tensors. In *Encyclopedia of Nuclear Magnetic Resonance*; Grant, D. M., Harris, R. K., Eds.; John Wiley & Sons: Chichester, U.K., 1996; Vol. 2, pp 1298−1321.
(44) Jameson, A. K.; Jameson, C. J. *Chem. Phys. Lett.* **1987**, *134*, 461−466.
(45) Sherwood, M. H. Chemical Shift Tensors in Single Crystals. In *Encyclopedia of Nuclear Magnetic Resonance*; Grant, D. M., Harris, R. K., Eds.; John Wiley & Sons: Chichester, U.K., 1996; Vol. 2, pp 1322−1330.
(46) Wasylishen, R. E. Dipolar and Indirect Coupling Tensors in Solids. In *Encyclopedia of Nuclear Magnetic Resonance*; Grant, D. M., Harris, R. K., Eds.; John Wiley & Sons: Chichester, U.K., 1996; Vol. 3, pp 1685−1695.
(47) Wasylishen, R. E. Indirect Nuclear Spin−Spin Coupling Tensors. In *Encyclopedia of Nuclear Magnetic Resonance*; Grant, D. M., Harris, R. K., Eds.; John Wiley & Sons: Chichester, U.K., 2002; Vol. 9, pp 274−282.
(48) Kaski, J.; Lantto, P.; Vaara, J.; Jokisaari, J. *J. Am. Chem. Soc.* **1998**, *120*, 3993−4005.

as the *z* axis of a reference frame and report the Euler angles[49] that rotate this reference frame into the pair of magnetic-shielding tensor PASs. These Euler angles are chosen such that after the transformation, the reference *z* axis becomes coincident with δ_{33}, the reference *y* axis lies along δ_{22}, and the reference *x* axis becomes parallel to δ_{11}. The convention used here is three successive right-handed rotations about the reference *z* axis (α), the new y' axis this generates (β), and the z'' axis that was generated by the first two rotations (γ).

3. Experimental Section

3.1. Sample Preparation. A sample of DPA at natural isotopic abundance was acquired commercially (Aldrich) and used without further purification. Diphenylacetylene-α,β-$^{13}C_2$ was prepared from *trans*-stilbene-α,β-$^{13}C_2$ (MSD Isotopes, 99% ^{13}C) according to standard techniques (see, for example, ref 50). The labeled diphenylacetylene so produced was characterized by both its melting point (59−60 °C) and solution ^{13}C NMR spectroscopy. Both (η^2-diphenylacetylene-α,β-$^{13}C_2$)Pt(PPh_3)$_2$ and its counterpart of natural isotopic abundance were prepared under a nitrogen atmosphere from the corresponding diphenylacetylene according to literature procedures.[51] Both natural isotopic abundance and $^{13}C_2$-labeled PtDPA were characterized by solution ^{13}C and ^{31}P NMR spectra (vide infra). Crystals of PtDPA suitable for X-ray analysis were grown by slow cooling from acetone, while the benzene and dichloromethane solvates were grown by slow cooling from the respective pure solvents. The polycrystalline powder samples of PtDPA·C_6H_6 used for the SSNMR experiments were prepared by recrystallization from a 7:3 acetone/benzene mixture.

3.2. X-ray Crystallography. Complete structures of PtDPA, PtDPA·C_6H_6, and PtDPA·CH_2Cl_2 were determined from studies of single crystals. The crystallographic data presented herein were recorded on a Bruker PLATFORM/SMART 1000 CCD diffractometer at −80 °C using graphite-monochromated Mo Kα radiation (λ = 0.71073 Å). The structural models were refined to the data with a full-matrix least-squares method on F^2 using the SHELXL-93 computer program.[52] Before analysis, an absorption correction was applied to the data using the software packaged with the diffractometer. Details of the structure solution and refinement, along with perspective views of the molecules showing thermal ellipsoids, have been deposited as Supporting Information. Complete tabulations of atomic coordinates, bond lengths, angles, and thermal parameters for all three structures are available in CIF format.

3.3. NMR Spectroscopy. Proton-decoupled ^{13}C and ^{31}P NMR spectra of natural isotopic abundance and ^{13}C-labeled PtDPA dissolved in CD_2Cl_2 (approximately 0.1 M) were acquired on a Varian Unity 500 NMR spectrometer. Peaks in the ^{13}C NMR spectra were referenced to neat liquid TMS at 0.0 ppm by setting the solvent ^{13}C peak to 53.8 ppm; those for the ^{31}P NMR spectra were referenced to an external 85% H_3PO_4(aq) sample at 0.0 ppm. The presence of ^{13}C NMR peaks from the 48 phenyl carbons in ^{13}C spectra of PtDPA overlapping with the alkynyl carbon peaks makes direct analysis intractable. As a simplifying treatment, contributions to spectra of the $^{13}C_2$-labeled samples from isochronous aromatic ^{13}C nuclei were removed by subtracting the spectra of a sample at natural isotopic abundance. Carbon-13 and phosphorus-31 NMR spectra of the $^{13}C_2$-labeled samples were simulated using the SIMPSON program.[53]

SSNMR spectra were acquired using variable-amplitude cross polarization,[54] under the Hartmann−Hahn matching condition,[55−57] and high-power ^1H decoupling during acquisition. Carbon-13 SSNMR spectra of solid DPA samples were obtained on Chemagnetics CMX Infinity 200 and Bruker AMX-400 NMR spectrometers using contact times of 2 ms and ^1H $\pi/2$ pulses of 3.0 to 4.0 μs combined with 10−20 s recycle delays. SSNMR spectra of ^{13}C and ^{31}P nuclei in PtDPA were obtained on Bruker Avance 300 and 500 MHz NMR systems using TPPM ^1H decoupling during acquisition.[58] Proton $\pi/2$ pulses of 4.0 μs were used while 6 ms contact times and recycle delays of 30−60 s were implemented. The ^{13}C NMR spectra were referenced to TMS with an MAS experiment through assignment of the high-frequency peak of an adamantane spectrum to 38.56 ppm.[59] The ^{31}P NMR spectra were referenced to 85% H_3PO_4(aq) by setting the lone peak (under MAS conditions) of solid $NH_4H_2PO_4$ to +0.81 ppm.[60] Contributions to ^{13}C NMR spectra of stationary samples from the aromatic ^{13}C nuclei at natural abundance were subtracted as described above, yielding spectra from only alkynyl carbons. The magnitude of the correction necessary for MAS experiments was reduced through use of the dipolar-dephasing experiment which depresses the signal from carbon nuclei in methine or methylene environments.[61] Spectra of the $^{13}C_2$-labeled samples were simulated with the WSOLIDS package (stationary samples)[62] or the SIMPSON program (samples undergoing MAS).[53]

3.4. DFT Calculations. Calculations of the alkynyl carbon magnetic-shielding tensors for DPA used a structural model based on data obtained from an X-ray study at 293 K.[63] We applied the Amsterdam Density Functional suite of programs (ADF 2004.01),[64−66] including the effects of an applied magnetic field with the NMR module,[35−37,67,68] which makes use of gauge-including atomic orbitals (GIAOs).[69,70] The functional employed contains the local-

(49) Rose, M. E. *Elementary Theory of Angular Momentum*; John Wiley & Sons: New York, 1967; p 50.
(50) Fieser, L. F.; Williamson, K. L. *Organic Experiments*, 5th ed.; D. C. Heath: Lexington, MA, 1983.
(51) Blake, D. M.; Roundhill, D. M. *Inorg. Synth.* **1978**, *18*, 120−124.
(52) Sheldrick, G. M. *SHELXL-93, A Program for Crystal Structure Determination*; University of Göttingen: Göttingen, Germany, 1993.
(53) Bak, M.; Rasmussen, J. T.; Nielsen, N. C. *J. Magn. Reson.* **2000**, *147*, 296−330.
(54) Peersen, O. B.; Wu, X.; Kustanovich, I.; Smith, S. O. *J. Magn. Reson., Ser. A* **1993**, *104*, 334−339.
(55) Hartmann, S. R.; Hahn, E. L. *Phys. Rev.* **1962**, *128*, 2042−2053.
(56) Pines, A.; Gibby, M. G.; Waugh, J. S. *J. Chem. Phys.* **1972**, *56*, 1776−1777.
(57) Pines, A.; Gibby, M. G.; Waugh, J. S. *J. Chem. Phys.* **1973**, *59*, 569−590.
(58) Bennett, A. E.; Rienstra, C. M.; Auger, M.; Lakshmi, K. V.; Griffin, R. G. *J. Chem. Phys.* **1995**, *103*, 6951−6958.
(59) Earl, W. L.; VanderHart, D. L. *J. Magn. Reson.* **1982**, *48*, 35−54.
(60) Bryce, D. L.; Bernard, G. M.; Gee, M.; Lumsden, M. D.; Eichele, K.; Wasylishen, R. E. *Can. J. Anal. Sci. Spectrosc.* **2001**, *46*, 46−82.
(61) Opella, S. J.; Frey, M. H. *J. Am. Chem. Soc.* **1979**, *101*, 5854−5856.
(62) Eichele, K.; Wasylishen, R. E. *WSOLIDS*, version 2.0.18; University of Alberta: Edmonton, Canada, 2000.
(63) Zanin, I. E.; Antipin, M. Y.; Struchkov, Y. T. *Sov. Phys. Crystallogr. (Engl. Transl.)* **1991**, *36*, 219−224; *Kristallografiya* **1991**, *36*, 411−419.
(64) ADF, version 2004.01; SCM, Theoretical Chemistry, Vrije Universiteit: Amsterdam, The Netherlands, 2004; http://www.scm.com.
(65) te Velde, G.; Bickelhaupt, F. M.; Baerends, E. J.; Fonseca Guerra, C.; van Gisbergen, S. J. A.; Snijders, J. G.; Ziegler, T. *J. Comput. Chem.* **2001**, *22*, 931−967.
(66) Fonseca Guerra, C.; Snijders, J. G.; te Velde, G.; Baerends, E. J. *Theor. Chem. Acc.* **1998**, *99*, 391−403.
(67) Wolff, S. K.; Ziegler, T.; van Lenthe, E.; Baerends, E. J. *J. Chem. Phys.* **1999**, *110*, 7689−7698.
(68) Wolff, S. K.; Ziegler, T. *J. Chem. Phys.* **1998**, *109*, 895−905.
(69) Ditchfield, R. *Mol. Phys.* **1974**, *27*, 789−807.
(70) Wolinski, K.; Hinton, J. F.; Pulay, P. *J. Am. Chem. Soc.* **1990**, *112*, 8251−8260.

density approximation of Vosko, Wilk, and Nusair,[71] as well as the nonlocal exchange correction of Becke[72] and the nonlocal correlation correction of Perdew.[73,74] Calculations used the vendor-supplied TZP basis set consisting of Slater-type orbitals which are of triple-ζ, single-polarization flexibility in the valence (double-ζ core). The calculated magnetic-shielding data were converted to chemical shifts (referenced to TMS) according to eq 1. We also calculated the alkenyl carbon shielding tensors for ethylene using the geometry of Duncan[75] and for *trans*-stilbene using the structure of the nondisordered site from the study of Harada and Ogawa.[76]

Calculations of the alkynyl carbon shielding tensors for PtDPA used the same method as for DPA, but relativistic effects[31] were included through two different theoretical methods. All-electron calculations used the relativistic version of the TZP basis set and the zeroth-order regular approximate Hamiltonian,[77,78] including both spin−orbit coupling and scalar relativistic effects (ZORA-DFT). Calculations of PtDPA without a relativistic Hamiltonian used the nonrelativistic version of the TZP basis set but with a frozen core on platinum (frozen at the 4f level and below). The structural model used in all calculations of PtDPA was obtained from the X-ray structure of the benzene solvate, where for reasons of efficiency, PPh_3 moieties were replaced with PMe_3 ligands. Methyl carbons for PMe_3 were fixed at the position of the phenyl-ring ipso carbons, and proton positions were set with idealized bond lengths of 1.089 Å and tetrahedral angles.

The alkynyl carbon shielding tensors of the model compound (η^2-acetylene)Pt(PMe_3)$_2$ were also calculated with the frozen-core method described above for PtDPA. In this case, the EPR/NMR module was applied to analyze the magnetic shielding tensor in terms of individual molecular-orbital contributions.[35−37] The structure of (η^2-acetylene)Pt(PMe_3)$_2$ was first optimized, under the constraint of C_{2v} symmetry, using the same nonrelativistic Hamiltonian and frozen-core basis set as the shielding calculations.

4. Results and Discussion

4.1. Diphenylacetylene-α,β-$^{13}C_2$. 4.1.1 Crystal Structure and Solid-State ^{13}C NMR Spectra. Before the results of ^{13}C NMR studies on DPA are discussed, it is worthwhile to first consider its solid-state structure as the symmetry is reflected in the NMR observations. The most recent structural examination found two symmetry-unique molecules per unit cell, but our SSNMR data do not distinguish the pair.[63] The source of this may be that, while the two molecules are formally different, all chemically equivalent C,C bonds in the two were found to be of equal length when atomic motions were taken into account.[63] Also, the large angle librations about the long axis of the molecule may serve to further negate site differences.[63] As the two molecules of DPA each provide the same ^{13}C NMR frequency response within the resolution, the spectra will be discussed as if a single site is present. The inversion center relating the alkynyl carbon nuclei requires that the two exhibit identical chemical shift tensors and thus form an A_2 spin system at every orientation in the magnetic field. While the only requirement of the space group on the molecular symmetry is this inversion center, there is very little deviation from D_{2h} symmetry.[63] Assuming an effective D_{2h} symmetry, the PAS of the alkynyl carbon CS tensor must be oriented such that one principal component is perpendicular to the plane of the molecule, another along the alkynyl bond, and the final component in the plane of the molecule but perpendicular to the alkynyl bond.

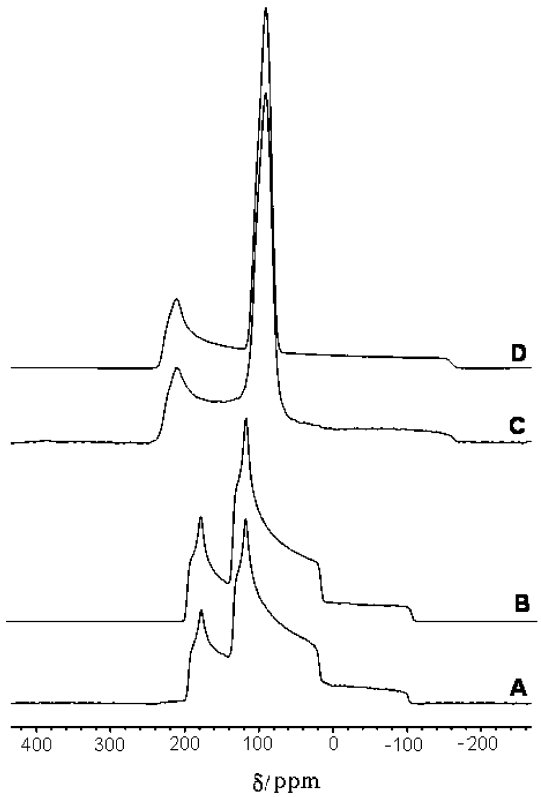

Figure 1. Simulated and experimental ^{13}C NMR spectra of the alkynyl carbons from stationary samples of DPA. Experimental spectra were recorded at applied field strengths of 9.4 (A) and 4.7 (C) T. The corresponding simulations are presented as traces B and D.

The ^{13}C NMR spectra from a stationary powder sample of diphenylacetylene-α,β-$^{13}C_2$ obtained at 4.7 and 9.4 T are shown in Figure 1; Table 1 summarizes the data derived from the ^{13}C spectral simulations. While the line shape seen in Figure 1C appears to be unusual for a dipolar chemical-shift spectrum, this pattern has been observed before and comes from a cancellation effect in the orientation dependence of the shielding and dipolar coupling interactions for one of the transitions.[26,47] The best-fit simulated spectra yield a value of $R_{DD} = 4025 \pm 50$ Hz corresponding to a length of 1.236-(5) Å for the alkynyl bond. This NMR-derived bond length is ∼4% greater than the 1.192(4) Å measured via X-ray crystallography by Zanin et al.[63] Such an apparent lengthening is not unexpected as NMR-determined bond lengths are generally 1−4% larger than those measured by diffraction studies because of averaging from vibrational/librational

(71) Vosko, S. H.; Wilk, L.; Nusair, M. *Can. J. Phys.* **1980**, *58*, 1200−1211.
(72) Becke, A. D. *Phys. Rev. A* **1988**, *38*, 3098−3100.
(73) Perdew, J. P. *Phys. Rev. B* **1986**, *33*, 8822−8824.
(74) Perdew, J. P. *Phys. Rev. B* **1986**, *34*, 7406.
(75) Duncan, J. L. *Mol. Phys.* **1974**, *28*, 1177−1191.
(76) Harada, J.; Ogawa, K. *J. Am. Chem. Soc.* **2004**, *126*, 3539−3544.
(77) van Lenthe, E.; Baerends, E. J.; Snijders, J. G. *J. Chem. Phys.* **1993**, *99*, 4597−4610.
(78) van Lenthe, E.; Baerends, E. J.; Snijders, J. G. *J. Chem. Phys.* **1994**, *101*, 9783−9792.

Table 1. Experimental and Calculated Alkynyl Carbon Chemical Shift Tensors for Diphenylacetylene and (η^2-Diphenylacetylene)Pt(PPh_3)$_2$

	δ_{11}	δ_{22}	δ_{33}	δ_{iso}[a]	Ω[a]	α[b]	β	γ
				DPA				
exptl[c]	165	147	−42	89.8	207	0	0	0
calcd	181	160	−39	101	220	0	0	0
				PtDPA				
exptl[d]	226.5	142	23.5	130.6	203	0	85	78
	221	140	21.5	127.6	200	0	94	104
calcd	223	158	45	142	178	0	83	82
	222	154	44	140	178	2	80	101

[a] Chemical shift, δ_{iso}, and span, Ω, values are in ppm. [b] The angles α, β, and γ are in degrees; see text for Euler angle conventions. [c] Uncertainties are estimated to be ±0.2 ppm for δ_{iso}, ± 2 ppm for the principal components of the CS tensors, and ±3° for the angles. [d] Uncertainties are estimated to be ±0.2 ppm for δ_{iso}, ±3 ppm for the principal components of the CS tensors, ±5° for β and γ, and ±10° for α.

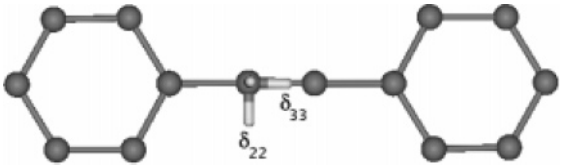

Figure 2. Principal axis system of the alkynyl carbon CS tensor of DPA. The unlabeled principal component directed out of the page is δ_{11}.

motion.[79−81] The isotropic chemical shift measured from the spectrum of the sample under MAS conditions, $\delta_{iso} = 89.8$ ppm, is consistent with the previously reported solvated sample value of 89.6 ppm.[82] Fits of simulated spectra to the data show that δ_{33} (−42 ppm) is along the alkynyl bond, but they do not distinguish which of δ_{11} (165 ppm) and δ_{22} (147 ppm) is perpendicular to the molecular plane and which is within it. DFT calculations (vide infra) suggest that δ_{11} is the component perpendicular to the molecular plane, as shown in Figure 2.

Alkynyl carbon CS tensors have previously been published for acetylene,[19,23] propyne,[23] 2-butyne,[23,24] diacetylene,[25] 2-butyne-1,4-diol,[26] methoxyacetylene,[27] propiolaldehyde,[27] trimethylsilylacetylene,[27] and phenylacetylene[28] (relaxation study). The CS tensor of DPA resembles that of the structurally similar phenylacetylene, whose terminal carbon has CS tensor components: $\delta_{33} = -27.8$ ppm and $\delta_{11} = \delta_{22} = 131.8$ ppm (values determined under the assumption that $\delta_{11} = \delta_{22}$).[28] The common characteristic of alkynyl carbon CS tensors is axial or near-axial symmetry, with the direction of greatest shielding along the alkynyl bond. The other two components, which are identical or similar, are in the plane perpendicular to the alkynyl bond and show much less effective shielding. The CS tensor of DPA conforms to the above pattern closely.

Several theoretical investigations into the origins of chemical shifts in alkynyl carbons have been published using either the Cornwell approximation[32−34] or the more sophisticated IGAIM method.[27,39] Examination of these analyses demonstrates that any substituents which do not affect the π-system of an acetylenic moiety will produce CS tensors very similar to those of the parent molecule, acetylene. Observe, for example, that the CS-tensor components of propyne and 2-butyne,[23] where the methyl substituents would not be expected to significantly affect the π-system, differ by a maximum of 15 ppm from those of acetylene.[19] Any more complicated π-system requires individual analysis because of the dependence of shielding on the structure and symmetry of the wave function. Even without such an analysis, it is the chemical shift along the alkynyl bond which will be most affected by the loss of a C_∞ axis. This is because it is only in the direction of a C_∞ axis that there is an identical lack of paramagnetic shielding terms.[83] For a detailed analysis of the effects of both substituents and an extended π-system, see the recent articles by Wiberg et al.[27,39] Theoretical studies of alkynyl carbon chemical shifts have also been undertaken by Moss and Goroff, who investigated complexation of iodoalkynes.[84] There has also been some discussion on the effects of phenyl-ring substituents on diphenylacetylene.[85]

4.1.2. DFT Chemical Shift Calculations. Given that the two symmetry nonequivalent DPA molecules are not distinguished by SSNMR, we chose only one for computational study. We selected the site for which all hydrogen atoms are recorded in the 293 K X-ray structure of Zanin et al.,[63] but we do not expect this selection to be pivotal considering the close structural similarities of the sites. The alkynyl carbon CS tensors (see Table 1) were calculated: they reproduce δ_{33} to within 3 ppm, while δ_{11} and δ_{22} are slightly less accurate, being 16 and 13 ppm too large. The calculated CS tensor places δ_{33} along the alkynyl bond in agreement with the experiment, and the calculated orientations of δ_{11} and δ_{22} are as shown in Figure 2.

4.2. (η^2-Diphenylacetylene-α,β-$^{13}C_2$)Pt(PPh_3)$_2$. 4.2.1 Crystal Structure. In 1967 a preliminary report on the structure of PtDPA was issued containing unit-cell parameters, as well as the bond lengths and angles, for the phosphorus, platinum, alkynyl carbon, and ipso phenyl carbon atoms.[22] Apparently the investigation was hindered by the existence of both monoclinic and triclinic forms,[8] which, in light of the present results was likely the result of the inclusion of solvent molecules in the crystals (vide infra). The 1967 study reported that the compound crystallizes in the triclinic space group $P\bar{1}$ with the following unit-cell parameters: a = 11.32(5) Å, b = 15.83(5) Å, c = 13.34(5) Å, α = 112.9(3)°, β = 113.4(3)°, γ = 83.7(3)°. While the authors do not state the solvent of crystallization, we find this to be an important factor for PtDPA. From acetone, we also found that the crystallites exhibited the symmetry of space group $P\bar{1}$ but with differing unit-cell parameters (see Table 2). While the values are significantly different, given the preliminary nature of the 1967 report as well as the lack of preparatory information, a direct comparison may not be valid. When using benzene as a mother liquor, we found that a 1:1 solvate

(79) Ishii, Y.; Terao, T.; Hayashi, S. *J. Chem. Phys.* **1997**, *107*, 2760−2774.
(80) Nakai, T.; Ashida, J.; Terao, T. *Mol. Phys.* **1989**, *67*, 839−847.
(81) Millar, J. M.; Thayer, A. M.; Zax, D. B.; Pines, A. *J. Am. Chem. Soc.* **1986**, *108*, 5113−5116.
(82) Kalinowski, H.-O.; Berger, S.; Braun, S. *Carbon-13 NMR Spectroscopy*; John Wiley & Sons: Chichester, U.K., 1988; p 162.
(83) Ramsey, N. F. *Phys. Rev.* **1950**, *78*, 699−703.
(84) Moss, W. N.; Goroff, N. S. *J. Org. Chem.* **2005**, *70*, 802−808.
(85) Rubin, M.; Trofimov, A.; Gevorgyan, V. *J. Am. Chem. Soc.* **2005**, *127*, 10243−10249.

Table 2. Crystallographic Data for (η^2-Diphenylacetylene)Pt(PPh_3)$_2$ and Solvates

	PtDPA	PtDPA·C_6H_6	PtDPA·CH_2Cl_2
formula	$C_{50}H_{40}P_2Pt$	$C_{56}H_{46}P_2Pt$	$C_{51}H_{42}Cl_2P_2Pt$
cryst syst	triclinic	monoclinic	monoclinic
space group	$P\bar{1}$	$P2_1/n$	$P2_1/n$
a (Å)	13.3195(8)	13.2507(7)	11.7140(8)
b (Å)	16.6524(9)	16.5061(9)	15.250(1)
c (Å)	18.304(1)	20.496(1)	23.707(2)
α (deg)	81.101(1)	90	90
β (deg)	87.024(1)	101.891(1)	91.847(2)
γ (deg)	77.930(1)	90	90
Z	4	4	4
unique molecules	2	1	1
R1 [$F_o^2 \geq 2\sigma(F_o^2)$][a]	0.0233	0.0295	0.0223
wR2 [all data][b]	0.0584	0.0653	0.0571

[a] $R1 = \Sigma||F_o| - |F_c||/\Sigma|F_o|$. [b] $wR2 = [\Sigma w(F_o^2 - F_c^2)^2/\Sigma w(F_o^4)]^{1/2}$.

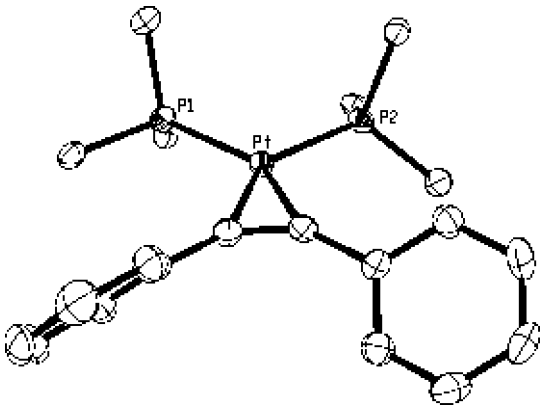

Figure 3. ORTEP[97] plot of PtDPA·C_6H_6 (50% probability ellipsoids) with the hydrogen atoms and all but the ipso carbons of the PPh_3 phenyl rings removed for clarity.

was formed, crystals of which have the symmetry properties of monoclinic space group $P2_1/n$ (alternate setting of $P2_1/c$). Crystals could also be grown as solvates from dichloromethane, and these too crystallized in $P2_1/n$. Important structural features of the three forms we have observed are summarized in Table 2. We list full details of the $P\bar{1}$ structure, as well as the benzene and dichloromethane solvates, in Supporting Information.

Because the SSNMR results are for the benzene solvate complex, and there are only minor differences in bond lengths and angles in the different forms, we limit further discussion and data to PtDPA·C_6H_6 only. The structure displayed in Figure 3 shows that the immediate coordination sphere of platinum displays a highly distorted square-planar geometry. The alkynyl carbons, which were related by an inversion center in DPA, are crystallographically independent. The two phosphorus nuclei are also unrelated by any symmetry operation. Upon coordination to the metal, the alkynyl bond of diphenylacetylene is elongated from 1.197 (and 1.198) Å to 1.280(5) Å. The linear geometry along the triple bond is also lost, with the ipso carbons of the phenyl rings bent back from the unsaturated C,C bond vector by 37.4(3) and 37.7(3)°. The phenyl rings of the diphenylacetylene ligand are also twisted out of the plane (in opposite directions). The Pt,C bonds are 2.047(3) and 2.048(3) Å, and the C−Pt−C angle is 36.4(1)°. All structural parameters are similar to those previously reported for (η^2-PhC≡CMe)-Pt(PPh_3)$_2$.[86]

Table 3. Literature and Experimental ^{13}C and ^{31}P NMR Parameters of (η^2-Diphenylacetylene)Pt(PPh_3)$_2$

parameter[a]	solvated[b]	literature[c]	MAS[d]
$\delta_{iso}(^{13}C_A)$ (ppm)	127.145(5)	127.9	127.6(2)
$\delta_{iso}(^{13}C_B)$ (ppm)			130.6(2)
$^1J(^{195}Pt,^{13}C_A)$ (Hz)	301.1(4)	299	265(15)
$^1J(^{195}Pt,^{13}C_B)$ (Hz)			285(15)
$^2J(^{31}P_{trans},^{13}C_A)$ (Hz)	68.7(4)	*e*	60(10)
$^2J(^{31}P_{trans},^{13}C_B)$ (Hz)			60(10)
$^2J(^{31}P_{cis},^{13}C)$ (Hz)	7.1(4)	*e*	
$^1J(^{13}C,^{13}C)$ (Hz)	85.7(4)		87(10)
$\delta_{iso}(^{31}P_A)$ (ppm)	28.090(5)	27.2	30.4(1)
$\delta_{iso}(^{31}P_B)$ (ppm)			26.1(1)
$^2J(^{31}P,^{31}P)$ (Hz)	31.8(4)		
$^1J(^{195}Pt,^{31}P_A)$ (Hz)	3454.2(4)	3445	3510(30)
$^1J(^{195}Pt,^{31}P_B)$ (Hz)			3380(30)

[a] All ^{13}C parameters refer to the alkynyl carbons. See text for discussion of the signs of these parameters. [b] Dissolved in CD_2Cl_2. [c] Data from the study of Boag et al.[8] [d] Solid sample is PtDPA·C_6H_6. [e] See text.

4.2.2. Solution ^{13}C NMR Spectra. The ^{13}C NMR spectrum of PtDPA dissolved in CD_2Cl_2 (Supporting Information) was analyzed to produce the data shown in Table 3, where the information previously reported by Boag et al. is also reproduced for convenience.[8] The present use of doubly ^{13}C-labeled PtDPA provides information beyond that available in the earlier study. All parameters found from the solution ^{13}C NMR spectra are in good agreement with prior data. We note that the DPA ligand slowly dissociates in CD_2Cl_2, as peaks from PtDPA (centered at 127 ppm) lost intensity over time such that no signal from the complex was detectable in the ^{13}C NMR spectrum after 24 h. Furthermore, a signal of increasing intensity from unbound DPA at 89.581(5) ppm was observed. These effects in the spectra are not indicative of fast exchange however, as both $^1J(^{195}Pt,^{13}C)$ and $^2J(^{31}P,^{13}C)$ are observed. The compound appears stable in the solid form however, as samples of the benzene solvate packed into standard rotors exhibited no changes in the ^{13}C or ^{31}P NMR spectra over the course of several months.

The peaks from the ^{195}Pt-containing isotopomers (33.8%) are conveniently separated by the large magnitude of $^1J(^{195}Pt,^{13}C)$ thus yielding this parameter, 301.1 Hz, separately. This value is typical for $^1J(^{195}Pt,^{13}C)$ in Pt(0) complexes; further values including those for Pt(II) complexes can be found in refs 4 and 6, but take note of Boag et al.'s word of caution[8] about errors in previous reports for the compounds (η^2-MeC≡CMe)Pt(PPh_3)$_2$ and *trans*-[PtMe(MeC≡CMe)(PMe_2Ph)$_2$][PF_6].

Carbon-13 NMR signals from the alkynyl carbons allow the *J* couplings with phosphorus-31 to be elucidated. The isotopomers that do not contain ^{195}Pt constitute an AA′XX′ spin system,[87,88] spectral analysis of which shows that the cis and trans $^2J(^{31}P,^{13}C)$ couplings are of opposite sign and

(86) Davies, B. W.; Payne, N. C. *J. Organomet. Chem.* **1975**, *99*, 315−328.
(87) Günther, H. *Angew. Chem., Int. Ed. Engl.* **1972**, *11*, 861−948.
(88) Günther, H. *NMR Spectroscopy: Basic Principles, Concepts, and Applications in Chemistry*, 2nd ed.; John Wiley & Sons: Chichester, U.K., 1995; pp 181−194.

have magnitudes of 68.7 and 7.1 Hz. The opposing signs of these terms makes their sum ±61.6 Hz, in close agreement with the value of ±61 Hz reported by Boag et al.[8] The larger of these values is assigned to the trans coupling as is usually done for the analogous alkene complexes of platinum.[89] Also, Wrackmeyer has shown that the sum $^2J(^{31}P_{cis},^{13}C) + {}^2J(^{31}P_{trans},^{13}C)$ is positive for $(\eta^2\text{-}C_2H_4)Pt(PPh_3)_2$,[89] so it follows that for PtDPA the larger (trans) value of 68.7 Hz is positive and the smaller (cis) coupling of 7.1 Hz is negative. Analysis of the AA′ XX′ spectrum also shows that $^1J(^{13}C,^{13}C)$ has the value of either 85.7 or 31.8 Hz and $^2J(^{31}P,^{31}P)$ has the other, but it does not yield the relative signs of these two couplings.[87,88] The value of ±31.8 Hz has been assigned to $^2J(^{31}P,^{31}P)$ given the similar magnitude to the 27 Hz reported for $(\eta^2\text{-PhC}{\equiv}\text{CPh})Pt(PMe_3)_2$[8] and the range of 35−56 Hz reported by Chaloner et al. for $^2J(^{31}P,^{31}P)$ in a series of asymmetrical $(\eta^2\text{-alkene})Pt(PPh_3)_2$ complexes.[7] Thus, the value of $^1J(^{13}C,^{13}C)$ for PtDPA in solution is ±85.7 Hz, significantly less than that expected for an alkyne. For comparison, in acetylene $^1J(^{13}C,^{13}C)$ is 171.5 Hz, in ethylene it is 67.6 Hz, and in ethane the coupling is 34.6 Hz.[90]

4.2.3. Solution and Solid-State MAS ^{31}P NMR Spectra. Analysis of the solution ^{31}P NMR spectrum of doubly ^{13}C-labeled PtDPA is identical to the ^{13}C case, but it now yields the δ_{iso} and ^{195}Pt coupling of ^{31}P. The data determined from this spectrum are also reported in Table 3. The value of $^1J(^{195}Pt,^{31}P) = 3454.2$ Hz is expected to be positive, as has been found in a large series of platinum phosphine complexes.[91,92]

For SSNMR studies, samples in which crystal symmetry dictates that there is only one unique molecule yield NMR spectra that are much simpler to analyze than those with more. Our NMR investigations were therefore focused on the solvate complexes, with the benzene solvate chosen for its expected lower volatility. However, given the similar bond lengths and angles in each form, we expect the results reported here to apply to each form without significant changes. Further, preliminary spectra of what was likely the solvent-free form are consistent with only minor changes from the currently reported data.[10] With the lower intrinsic resolution of SSNMR, the smaller couplings observed in solution spectra, $^2J(^{31}P,^{13}C)$ and $^2J(^{31}P,^{31}P)$, are not resolved, and each phosphorus site produces a signal at its isotropic shift as well as from the AX spin pair with ^{195}Pt. The parameters from the SSNMR spectrum are similar to the values observed in solution and are listed in Table 3. The simplicity of the solid-state spectrum is indicative of a single symmetry-unique molecule and thereby confirms that the powder was composed of the benzene solvate. ^{31}P SSNMR was therefore used before and after all ^{13}C SSNMR measurements as a confirmation of purity.

4.2.4. Solid-State ^{13}C NMR Spectra. The ^{13}C NMR spectrum from the alkynyl carbons of PtDPA·C_6H_6 under MAS conditions is shown in Figure 4. Overlapping peaks from natural-abundance carbon nuclei were first removed (vide supra), and all spinning sidebands were added into the isotropic peak to mimic an infinite-spinning rate experiment. Best-fit parameters are shown in Table 3, and the spectrum simulated using these data is also presented in Figure 4. This same figure further displays the component subspectra from the contributing isotopomers. Nonquantitative matching of the simulation intensities to the central two peaks is attributed to the natural-abundance carbon correction which is largest in this region. These simulations were invariant to the value of $^2J(^{31}P_{cis},^{13}C)$ if this quantity is less than twice the value measured in solution. We also note that in this case, the relative signs of the *J* couplings do not manifest themselves in the solid-state NMR spectrum. All parameters are found to be quite similar to those measured for PtDPA dissolved in CD_2Cl_2.

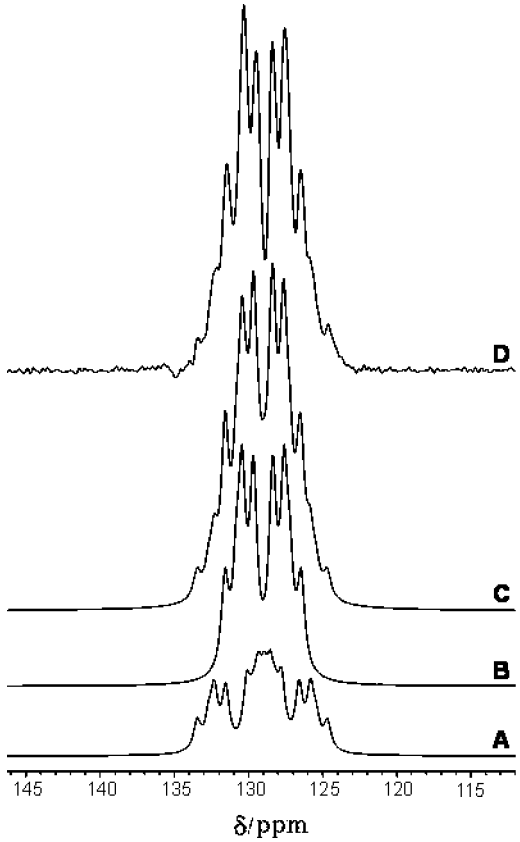

Figure 4. Simulated and experimental ^{13}C NMR spectra of the alkynyl carbons from PtDPA at 7.05 T, acquired with MAS (ν_{rot} = 8 kHz). Simulated spectra are shown with (A) and without (B) ^{195}Pt (I = 1/2, N. A. = 33.8%). The sum of the subspectra is also shown (C) for comparison with the experimental spectrum (D).

Both calculated and experimental ^{13}C NMR spectra of stationary samples of $^{13}C_2$-labeled samples of PtDPA are shown in Figure 5. There is some residual noise in the experimental line shapes from imperfect subtraction of the natural-abundance ^{13}C signals. The 20−30 kHz broad powder patterns are not likely to be significantly affected by the less than 0.3 kHz couplings involving phosphorus-31 or the less than 0.8 kHz couplings involving platinum-195, particularly given the 33.8% natural abundance of ^{195}Pt. The system was therefore treated as an isolated AB spin pair of carbon-13

(89) Wrackmeyer, B. *Z. Naturforsch. B* **1997**, *52*, 1019−1021.
(90) Lynden-Bell, R. M.; Sheppard, N. *Proc. R. Soc. London, Ser. A* **1962**, *269*, 385−403.
(91) McFarlane, W. *J. Chem. Soc. A* **1967**, 1922−1923.
(92) Anderson, D. W.; Ebsworth, E. A. V.; Rankin, D. W. H. *J. Chem. Soc., Dalton Trans.* **1973**, 2370−2373.

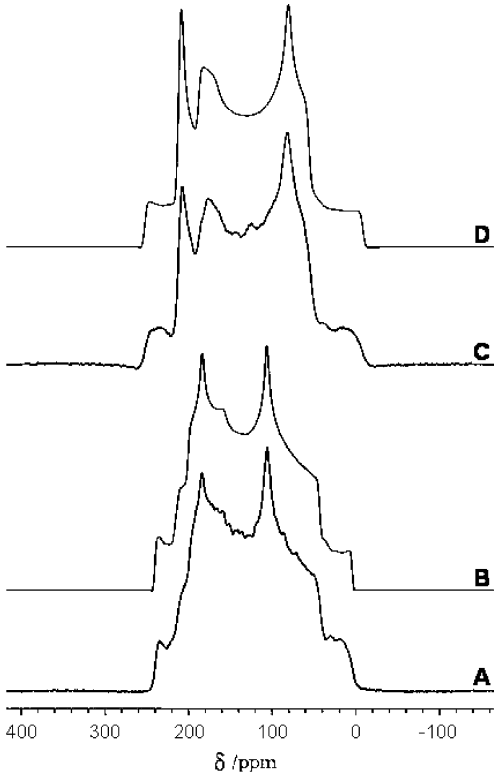

Figure 5. Simulated and experimental ^{13}C NMR spectra of the alkynyl carbons from stationary samples of PtDPA. Experimental spectra were recorded at applied field strengths of 11.75 (A) and 7.05 (C) T. The corresponding simulations are presented as traces B and D.

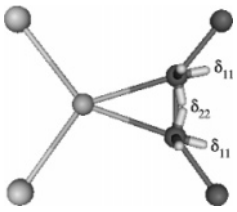

Figure 6. Principal axis systems for the alkynyl carbon CS tensors of PtDPA. δ_{11} and δ_{22} are labeled, while δ_{33} is directed out of the page. For clarity, all phenyl rings are removed except for the ipso carbons of the diphenylacetylene rings.

nuclei, and the chemical shift parameters derived from simulation are summarized in Table 1. Spectral simulations yield a value of 3250 ± 50 Hz for R_{DD} leading to an NMR-derived alkynyl C,C bond length of 1.327(7) Å, about 4% greater than that found by X-ray diffraction methods. As mentioned above, an apparent lengthening of such an order is expected from vibrational/librational effects. We further note that simulations of the spectra from stationary samples are insensitive to $^1J(^{13}C,^{13}C)$ in the range determined from the MAS experiment.

The orientations for the alkynyl carbon CS tensors of PtDPA are shown in Figure 6. As is shown there, the tensors are oriented such that δ_{22} is approximately along the alkynyl bond, δ_{33} is nearly perpendicular to the plane formed by platinum and the alkynyl carbons, and δ_{11} is approximately in the $Pt-C_2$ plane, orthogonal to the alkynyl bond. While this is one possible solution, the cylindrical symmetry of the dipolar interaction causes the spectral simulation to be invariant to simultaneous rotation of both tensors about the internuclear $^{13}C,^{13}C$ vector (in this case, the alkynyl bond).[16−21] All members of the solution set have δ_{22} approximately along the alkynyl bond, while δ_{33} and δ_{11} are perpendicular to it; therefore, these features are experimentally known. The absolute orientation of the tensors in the molecular framework can be determined if the dihedral angle between any one principal component and some other feature of the molecular geometry is found. Because the ZORA-DFT calculated CS tensors each have the δ_{11} principal component contained within the plane formed by the platinum and alkynyl carbon atoms, this orientation parameter was fixed, and all others seen in Figure 6 were generated from the experimental Euler angles. In this instance, there is no ambiguity introduced from a need to pair specific calculated and experimental tensors, because the same relative orientation is shared by each experimental (where $\alpha_1 - \alpha_2 = 0$) and calculated (where $\alpha_1 - \alpha_2 \approx 0$) CS tensor.

4.2.5. DFT Chemical Shift Calculations. Alkynyl carbon CS tensors of PtDPA were calculated using the all-electron ZORA-DFT method described above. A similar theoretical method, equivalent other than the relativistic Pauli Hamiltonian and the frozen-core basis required, has been shown to yield excellent results in a series of 5d transition metal carbonyls.[68] Both the calculated shifts and available orientation information are in good agreement with experiment (see Table 1), which gives confidence in the angular information that was used to affix the CS tensors in the molecule.

Some previously published studies of alkenes η^2-bonded to platinum proposed absolute alkenyl carbon CS tensor orientations based on $^{13}C,^{13}C$ dipolar chemical shift solid-state NMR data together with Hartree−Fock or DFT (B3LYP) calculations employing an effective core potential (ECP) at platinum to account for relativistic effects.[16,17] Given the success of the relativistic all-electron calculations on the present system, an evaluation of the validity of the previous ECP calculations of carbon shielding is possible. Calculations using a nonrelativistic Hamiltonian may fail to reproduce experimental observations for the following reasons: (a) absence of the spin−orbit contribution to shielding which occurs only with a relativistic formalism[31] or (b) lower quality of the zero-field wave function from the lack of a relativistic Hamiltonian. The spin−orbit contribution is <6 ppm in any direction, therefore effect (a) does not seem to be significant here. Given that relativistic effects are greatest for core electrons and ECP methods replace these with relativistically derived pseudopotentials, it may be expected that ECP calculations will correct for most of effect (b). Using a frozen-core treatment (vide supra), which is analogous to an ECP calculation, reproduces the the CS tensor with reasonable accuracy: $\delta_{11} = 226$ ppm, $\delta_{22} = 135$ ppm, $\delta_{33} = 68$ ppm. Furthermore, the orientations calculated with the two methods are qualitatively similar and when setting the final orientation of the experimental CS tensors as above, the two methods agree within 2 degrees. On the basis of these data, we find no reason to call into question the orientations proposed in earlier investigations through a combination of experiments and ECP calculations.[16,17]

4.3. Summary of the Effects of η^2-Bonding to Pt(0) on Unsaturated-Carbon CS Tensors. The effects of η^2-bonding to platinum on alkynyl carbon chemical shifts has previously been probed with isotropic chemical shift data derived from the spectra of solvated samples.[4] A consistent effect of decreased shielding has been observed, for example by Boag et al. who reported a coordination-induced deshielding of 31.4−43.8 ppm for a large series of acetylenes in platinum(0) complexes.[8] For a solvated sample, the coordination-induced deshielding for DPA forming PtDPA has been reported as 38.3 ppm,[8] similar to the 38 and 41 ppm values observed here in the solid state.

Determination of the orientation dependence of the alkynyl carbon CS tensors for both DPA and PtDPA (see Figures 2, 6, 7 and Table 1) provides a more complete picture than the isotropic data previously investigated. The CS tensor of DPA is nearly axially symmetric and is aligned such that the direction of greatest shielding is along the triple bond, while two nearly equal principal components (av = 155 ppm) are found perpendicular to the bond. Upon coordination with platinum, the chemical shift along the alkynyl bond, δ_{33} in DPA and δ_{22} in PtDPA, increases by nearly 200 ppm! Perpendicular to the C,C bond, bonding to platinum causes the chemical shift to increase by ~70 ppm in one direction (within the Pt−C_2 plane) but decrease by ~130 ppm in the other (perpendicular to the Pt−C_2 plane). It is particularly noteworthy that the chemical shift in directions perpendicular to the alkynyl bond is nearly the same in DPA (δ_{11} and δ_{22}) but varies by ~200 ppm in PtDPA (δ_{11} and δ_{33}). The net deshielding that has been observed upon coordination can now be seen to come from a cancellation effect due to a deshielding in two directions and an increased shielding in the third. When just the principal components are compared, δ_{22} is altered only slightly, while δ_{11} and δ_{33} are larger by approximately 60 ppm. However, consideration of the orientation information shows that δ_{22} of DPA is aligned perpendicular to the alkynyl bond, while it is nearly along the analogous bond in PtDPA. This reinforces the importance of analyzing chemical shift data utilizing not only the principal tensor components but also geometrical information.

The effect of complexation with platinum(0) on an alkynyl carbon CS tensor is different from what has been observed for alkenyl carbons. In PtDPA, there is a deshielding in two directions and an increase in shielding along the third. In the closest alkene analogue, *trans*-stilbene-forming (η^2-*trans*-stilbene)Pt(PPh_3)$_2$, coordination results in increased shielding in all directions.[17] A summary of the effects of bonding to platinum(0) on the CS tensors of alkynyl and alkenyl carbons is given in Figure 7.

4.4. A Comparison of the Alkynyl Carbon CS Tensors for (η^2-Diphenylacetylene)Pt(PPh_3)$_2$ and *trans*-Stilbene. The bonding of unsaturated-carbon ligands to late transition metals is commonly discussed in terms of the Dewar−Chatt−Duncanson (DCD) model, wherein donation of electron density to the π^*-type orbital of the ligand creates an

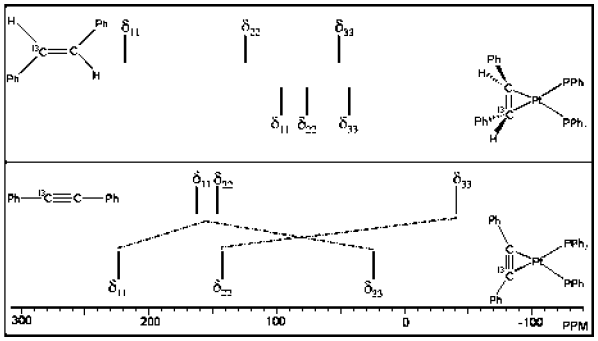

Figure 7. Summary of the effects on the CS tensors of the alkenyl and alkynyl carbons caused by η^2-bonding with platinum(0). In the diagram for DPA forming PtDPA, dashed lines link orientationally similar principal components.

effective double bond.[93] This model has provided effective arguments for the changes of such properties as bond lengths and vibrational frequencies of the ligand upon bonding to a transition metal. A key strength of the DCD model is that it is useful not only in property prediction but also in providing intuitive insight into bonding which has proven helpful in modifying reactivity (e.g., reactivity umpolung).[94] As magnetic shielding is an electronic property, it is interesting to evaluate its relationship to the DCD model. The obvious comparison for the alkynyl carbon CS tensor in PtDPA is *cis*-stilbene since the DPA ligand in PtDPA has a similar structure to that of *cis*-stilbene. Although the alkenyl carbon CS tensors for *cis*-stilbene are not known, they are not expected to be very different from those for *trans*-stilbene. This expectation is suggested by the fact that the principal components of the relevant carbon CS tensors for *cis*- and *trans*-2-butene do not differ by more than 15 ppm and have the same orientation in their respective molecular frameworks.[95] The averaged values for the principal components of the alkynyl carbon CS tensors of PtDPA, δ_{11} = 224 ppm, δ_{22} = 141 ppm, and δ_{33} = 22 ppm, are similar to those measured for uncoordinated *trans*-stilbene: δ_{11} = 215 ppm, δ_{22} = 120 ppm, and δ_{33} = 49 ppm.[17] The orientation of the CS tensor of *trans*-stilbene is such that δ_{33} is approximately perpendicular to the molecular plane, δ_{22} is nearly parallel to the alkenyl C,C bond, and δ_{11} is approximately in the molecular plane and orthogonal to the alkenyl bond, analogous to that of PtDPA (Figure 6). Not only are the CS tensors of the alkynyl carbons of PtDPA similar to those of *trans*-stilbene but the indirect coupling measured in solution ($^1J(^{13}C,^{13}C)$ = 85.7 Hz) is also of similar magnitude to that of *trans*-stilbene ($^1J(^{13}C,^{13}C)$ = 72.9 Hz).[96]

Given the observed similarity for the CS tensors of PtDPA and *trans*-stilbene (TSB), the question becomes whether there is an equivalent response to the operators that describe

(93) (a) Dewar, M. J. S. *Bull. Soc. Chim. Fr.* **1951**, *18*, C71. (b) Chatt, J.; Duncanson, L. A. *J. Chem. Soc.* **1953**, 2939−2947. (c) Nelson, J. H.; Wheelock, K. S.; Cusachs, L. C.; Jonassen, H. B. *J. Am. Chem. Soc.* **1969**, *91*, 7005−7008. (d) Nelson, J. H.; Jonassen, H. B. *Coord. Chem. Rev.* **1971**, *6*, 27−63.
(94) Seebach, D. *Angew. Chem., Int. Ed. Engl.* **1979**, *18*, 239−258.
(95) Zilm, K. W.; Conlin, R. T.; Grant, D. M.; Michl, J. *J. Am. Chem. Soc.* **1980**, *102*, 6672−6676.
(96) Hansen, P. E.; Poulsen, O. K.; Berg, A. *Org. Magn. Reson.* **1979**, *12*, 43.

magnetic shielding for TSB and the η^2-ligand in PtDPA. According to the DCD model, when analyzing the character (strength) of the alkynyl[5] bond in PtDPA, the important features of the wave function are occupied molecular orbitals (MOs) containing fragment orbitals from the η^2-segment of the organic ligand with σ, π_x, π_y, and π_y^* character. These fragment orbitals are interpreted to yield a net bond order of two between the carbons directly connected to platinum. However, since shielding depends on the entire MO (see Appendix), the fact that these fragment orbitals exist in MOs that are linear combinations with d orbitals on Pt becomes important. Since MO contributions from atomic orbitals at platinum need to be considered for shielding of the alkynyl[5] carbons in PtDPA, there is likely some difference from the contributions to shielding of the alkenyl carbons in TSB.

Magnetic shielding can be calculated as a sum of contributions, whose form varies with the theory used. Here we discuss shielding in terms of the method of Shreckenbach and Zeigler[35−37] (see Appendix). Within this formalism, we examine the $\sigma^{p,oc-vir}$ term to probe for similarities or differences in the carbon shielding of TSB and PtDPA because of its similarity to the Cornwell approximation used in a body of literature analyzing shielding contributions.[32−34] There is a contribution to the magnetic shielding, σ, from the coupling of each pairing of an occupied, ψ_i^{occ}, and virtual, ψ_j^{vir}, molecular orbital, and this contribution is labeled $\sigma_{ij}^{p,oc-vir}$. From the arguments presented in the appendix it is apparent that for PtDPA, the $\sigma_{ij}^{p,oc-vir}$ terms for the alkynyl[5] carbons will include matrix elements of the $\hat{l}_z$ operator between atomic orbitals at platinum. We now turn to the question of whether these matrix elements have a significant effect on the shielding.

To address this question, we investigated the alkynyl carbon[5] magnetic shielding tensor for the model system (η^2-acetylene)Pt(PMe_3)$_2$. DFT-GIAO calculation of magnetic shielding for the alkynyl[5] carbons yields chemical shift tensor components, $\delta_{11} = 213$ ppm, $\delta_{22} = 56$ ppm, and $\delta_{33} = 55$ ppm, and a tensor orientation analogous to that of PtDPA (Figure 6). This is a fitting model as we here analyze the δ_{33} component which is only 10 (11) ppm different from the calculated results for the title complex. An energy level diagram of the complex is shown in Figure 8, which also displays two of the molecular orbitals relevant to magnetic shielding in this complex, designated HOMO−5 and LUMO+1. The coupling of HOMO−5 with LUMO+1 produces a $\sigma_{ij}^{p,oc-vir}$ term of +45 ppm in the shielding perpendicular to the Pt−C_2 plane. In the appendix, it is shown how a positive $\sigma_{ij}^{p,oc-vir}$ term is unusual and furthermore how it originates in the structure of the occupied, ψ_i^{occ}, and virtual, ψ_j^{vir}, MOs away from the nucleus for which shielding is calculated. The two orbitals shown in Figure 8 have their largest contributions from atomic orbitals at Pt, and this is the origin of the positive sign of $\sigma_{ij}^{p,oc-vir}$ for carbon from these two MOs. It is particularly interesting that contributions to the MOs from the atomic orbitals of platinum cause a large positive $\sigma_{ij}^{p,oc-vir}$ shielding term for the alkynyl[5] carbons, as this is the opposite sign to the usual case. In fact,

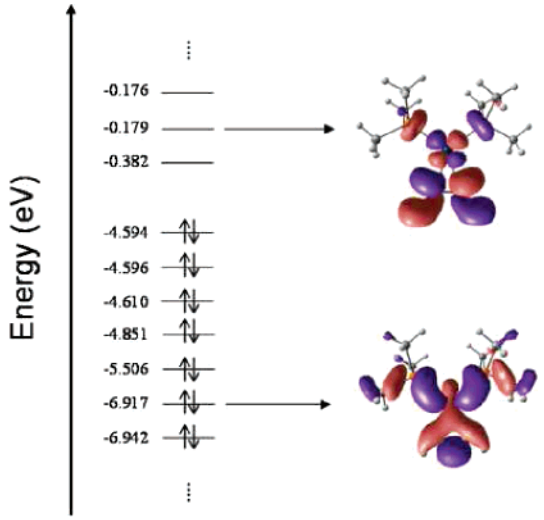

Figure 8. Abbreviated energy level diagram of the MOs of (η^2-acetylene)-Pt(PMe_3)$_2$ on a nonlinear energy scale. We label the orbitals counting down from the HOMO, and counting up from the LUMO. The plotted orbitals, HOMO−5 and LUMO+1, couple to produce a +45 ppm $\sigma_{ij}^{p,oc-vir}$ term directed out of the page for the alkynyl carbon magnetic shielding (see text).

DFT-GIAO calculations of the CS tensor for TSB ($\delta_{11} = 222$ ppm, $\delta_{22} = 124$ ppm, and $\delta_{33} = 30$ ppm with orientation matching the experimental results noted above) and for the parent compound ethylene ($\delta_{11} = 267$ ppm, $\delta_{22} = 113$ ppm, and $\delta_{33} = 15$ ppm with orientation analogous to TSB) show no positive contributions to $\sigma_{ij}^{p,oc-vir}$ perpendicular to the molecular plane greater than one-quarter that shown above for (η^2-acetylene)Pt(PMe_3)$_2$. There are a large number of significant $\sigma_{ij}^{p,oc-vir}$ terms, and many of these terms come from MOs that contain contributions from d orbitals at Pt. While the effect on each of these terms is likely not as dramatic as the HOMO−5 and LUMO+1 coupling discussed above, according to the arguments in the appendix, each term between MOs containing contributions from atomic orbitals at Pt will be modulated by these contributions. Since the structure of the wave function at the metal is important for the alkynyl carbon[5] shielding, it appears that the metallic complex responds differently to the operators that describe magnetic shielding than does an organic alkene.

The DCD model provides valuable insight into the nature of bonding in transition metal compounds. It is important, however, to carefully consider the implications of this model. Typical applications of the DCD model are an explanation of the change in C,C bond length or IR frequency upon complexation. Effectively, these are both measures of the bond order which is dependent on the structure of the MOs local to the unsaturated carbon bond, while the magnetic shielding is an involved probe of the total structure of the occupied and virtual MOs. Describing an alkynyl ligand bound to platinum as an effective double bond is using terminology that refers to the electronic structure local to the ligand, while the shielding is shown here to not be local to the ligand. It then appears fitting to conclude that the CS tensors of the alkynyl[5] carbons in PtDPA are similar to those of an alkene but not because the alkynyl bond becomes an effective double bond in the complex.

5. Conclusions

Previous studies of the orientation-dependent changes in alkenyl carbon CS tensors upon coordination with Pt(0) and Pt(II) have provided prototypes for understanding isotropic chemical shift differences caused by bonding to late transition metals.[16,17] Because of the consistent effect of bonding on isotropic chemical shifts in a series of alkynes and their platinum(0) coordination complexes,[8] we believe study of a representative alkyne would generally be applicable to the CS tensor changes from coordination of alkynes with late transition metals. To this end, alkynyl carbon chemical shift tensors of diphenylacetylene and (η^2-diphenylacetylene)Pt-$(PPh_3)_2$ have been characterized by ^{13}C NMR spectroscopy of solid samples. Orientations for the carbon CS tensors have been proposed on the basis of a combined experimental−theoretical approach. This information provides a more complete picture of the effect of η^2-bonding to Pt(0) on the NMR parameters of alkynes. Upon coordination to platinum, the carbon chemical shift in two directions becomes larger (less effective magnetic shielding), but in the remaining one, it becomes smaller (increased magnetic shielding). These competing effects lead to a net larger value for the isotropic shift as has been observed in solution NMR studies for the coordination of alkynes in Pt(0) compounds.[8] This directional dependence is in contrast to the effects of coordination on alkenyl carbon CS tensors, where formation of both Pt(0) and Pt(II) compounds causes the chemical shift to become smaller (more effective magnetic shielding) in all directions.[11−17] There exists a striking similarity between the orientation and principal component magnitudes of the alkenyl carbon CS tensors in *trans*-stilbene and those of the alkynyl carbons in PtDPA;[17] however, theoretical arguments demonstrate that the similarity is not the result of the η^2-carbons forming an effective double bond. DFT calculations are found to be accurate enough for assigning final ^{13}C CS tensor orientations and valuable for providing theoretical insights.

Acknowledgment. The authors thank the SSNMR group at the University of Alberta for many helpful discussions. We thank the Natural Sciences and Engineering Research Council (NSERC) of Canada for research grants supporting this work. Further funding was supplied through the Canada Research Chairs Program via a Research Chair in Physical Chemistry held by R.E.W. at the University of Alberta. K.J.H. thanks the University of Alberta for funding.

Appendix

To contrast the origins of carbon magnetic shielding for alkenes versus η^2-bonded alkynyl carbons, we provide the following short theoretical discussion. The original formulation for the calculation of magnetic shielding is the perturbation-theory expression of Ramsey which separates the shielding into diamagnetic and paramagnetic terms, $\sigma = \sigma^d + \sigma^p$.[83] The diamagnetic contribution contains terms only from the ground-state wave function, and while large, it varies little between compounds. Variations in the paramagnetic contribution are therefore responsible for nearly all of the difference in chemical shifts between compounds. Thus we focus on this term in comparing the shielding tensors of an alkene and platinum-bonded alkyne.

We briefly discuss the DFT-GIAO formalism for the calculation of magnetic shielding of Schreckenbach and Ziegler,[35,36] as it provides both accurate numerical results as well as the possiblity of deconvoluting the contributions to shielding. In this formulation, the paramagnetic term is further subdivided, $\sigma^p = \sigma^{p,oc-oc} + \sigma^{p,oc-vir} + \sigma^{p,rest}$, where $\sigma^{p,rest}$ is a "gauge invariance" term that is generally small, $\sigma^{p,oc-oc}$ comes from matrix elements between occupied MOs, and $\sigma^{p,oc-vir}$ is a term that involves matrix elements between occupied and virtual MOs. It is the $\sigma^{p,oc-vir}$ term that is informative in the present case, and its mechanism can be understood with relatively simple arguments in favorable cases. For a specific occupied, ψ_i^{occ}, and virtual, ψ_j^{vir}, molecular orbital (MO), the equation for this term is[35,36,98]

$$\sigma_{ij}^{p,oc-vir} = Ku_{ji}h_{ji}\Delta E_{ji}^{-1} \tag{3}$$

where K is a collection of constants and ΔE_{ji}^{-1} is the difference in energy between ψ_i^{occ} and ψ_j^{vir}. All equations given below for the elements of u_{ji} and h_{ji} will be for the shielding observed when the magnetic field is along the z axis. When expanding MOs in terms of atomic orbitals, AOs, we will use the notation χ_μ^s for basis function μ centered at s and $C_{\mu i}$ for the coefficient of this basis function in MO ψ_i. The operator for the z component of angular momentum will be given as $\hat{l}_z^s$ which indicates that this operator is centered at point s.

Several years ago, Schreckenbach and Ziegler pointed out that the leading contribution to u_{ji} is the sum (over all basis functions in ψ_i^{occ} and ψ_j^{vir}) of matrix elements with the form[35,36]

$$T_{\nu\mu} = C_{\nu j}C_{\mu i}\langle\chi_\nu^t|\hat{l}_z^s|\chi_\mu^s\rangle \tag{4}$$

The second term, h_{ji}, is the sum of matrix elements

$$U_{\nu\mu} = C_{\nu j}C_{\mu i}\left\langle\chi_\nu^t\left|\frac{\hat{l}_z^N}{r_N^3}\right|\chi_\mu^s\right\rangle \tag{5}$$

again over all basis functions in both the occupied and virtual orbitals. In h_{ji}, the $\hat{l}_z$ operator is centered at the magnetic nucleus,[32] N, and r_N^3 denotes the distance from the magnetic nucleus. We are interested in large changes in $\sigma_{ij}^{p,oc-vir}$, and therefore only need consider large terms. Since the $U_{\nu\mu}$ matrix elements fall off rapidly with distance from the magnetic nucleus, we exclude terms with atomic orbitals not from this nucleus (i.e., only terms with $t = s = N$ are kept for terms in h_{ji}). We also point out that as the $T_{\nu\mu}$ matrix elements in u_{ji} run over every atomic orbital that contributes to each of ψ_i^{occ} and ψ_j^{vir}, the magnitude of a given $\sigma_{ij}^{p,oc-vir}$ depends on

(97) Farrugia, L. J. *J. Appl. Crystallogr.* **1997**, *30*, 565.
(98) To make the u_{ji} and h_{ji} terms of congruent form, one term from eqs 3−22c of ref 36 is given but with constants combined in K and the energy difference term given explicitly rather than absorbed in u_{ji}.

the structure of the entire ψ_i^{occ} and ψ_j^{vir}, not just that at the magnetic nucleus.

Insight can also be gained into the sign of $\sigma_{ij}^{p,oc-vir}$ from the form of these equations through consideration of the relative signs of u_{ji} and h_{ji}. An important point to note is that because $1/r_N^3$ is everywhere positive, the sign of the $U_{\nu\mu}$ matrix elements are the same as those of the $T_{\nu\mu}$ matrix elements between the same basis functions. For example, if the MOs ψ_i^{occ} and ψ_j^{vir} are both composed of a single AO at *N*, there is only one $T_{\nu\mu}$ and one $U_{\nu\mu}$ term, and these have the same sign and imaginary character. With these example MOs, the equation for $\sigma_{ij}^{p,oc-vir}$ is formed such that a negative contribution will result. If we now consider adding to both of the MOs ψ_i^{occ} and ψ_j^{vir} an AO with a larger coefficient at a second atom, the sign of h_{ji} is unaltered because it includes only the contribution at the magnetic nucleus. The u_{ji} term however, can have a different sign because it is dominated by the larger contribution from an AO at a second atom. This simple example shows how large positive contributions to $\sigma_{ij}^{p,oc-vir}$ can occur when the occupied and virtual orbitals involved are dominated by AOs at other atoms in the molecule. The effect on the sign of the σ^p contributions for a given nucleus by dominating MO contributions at other atoms was first described by Cornwell in explaining the "anomalous" ^{19}F shielding of ClF,[32] and Cornwell's argument was later shown to apply to the ^{19}F shielding in BrF and IF.[99] Positive paramagnetic shielding terms have also been the subject of IGAIM calculations.[38]

Supporting Information Available: The ^{13}C NMR spectrum of (η^2-diphenylacetylene)Pt(PPh_3)$_2$ dissolved in CD_2Cl_2 (accompanied by spectral simulations), full crystal structures in CIF format, and crystallographic structure reports, including figures and tables, for (η^2-diphenylacetylene)Pt(PPh_3)$_2$, (η^2-diphenylacetylene)Pt(PPh_3)$_2$·(C_6H_6), and (η^2-diphenylacetylene)Pt(PPh_3)$_2$·(CH_2Cl_2). This material is available free of charge via the Internet at http://pubs.acs.org.

IC051548F

(99) Müller, H. S. P.; Gerry, M. C. L. *J. Chem. Phys.* **1995**, *103*, 577−583.